Toll, D. G. & Ong, B. H. (2003). *Géotechnique* **53**, No. 1, 93–103

Critical-state parameters for an unsaturated residual sandy clay

D. G. TOLL* and B. H. ONG†

This paper presents experimental data from constant water content triaxial tests on a residual soil from Singapore, tested under unsaturated conditions with measurements of matric suctions. The data for critical-state conditions from these tests are presented within a framework previously proposed by the first author. The unsaturated critical state requires five parameters: M_a, M_b, Γ_{ab}, λ_a and λ_b. At high degrees of saturation (in a non-aggregated condition) $M_a = M_b = M_s$ (the saturated critical-state stress ratio). At lower degrees of saturation, the value of M_b drops considerably and reaches values near to zero at degrees of saturation below 60%. Conversely, the value of M_a appears to increase as the degree of saturation reduces. A similar pattern is observed for λ_a and λ_b. The functions relating the critical-state parameters to degree of saturation (or volumetric water content) can be expressed in normalised form by referencing them to the saturated state. The same normalised functions for M_a/M_s, M_b/M_s, λ_a/λ_s and λ_b/λ_s fit the experimental data for the residual sandy clay from Singapore and a lateritic gravel from Kenya previously tested. This suggests that the form of these functions may be common to a range of soil types.

KEYWORDS: compressibility; fabric/structure of soils; partial saturation; residual soils; shear strength; suction

Cet exposé présente les résultats expérimentaux d'essais triaxiaux á teneur en eau constante sur un sol résiduel de Singapour, testé dans des conditions non saturées avec prises de mesures des succions matricielles. Dans le cadre de travail proposé par Toll (1990), nous présentons les données provenant de ces tests et relatives aux conditions d'état critique. L'état critique non saturé demande cinq paramètres M_a, M_b, Γ_{ab}, λ_a et λ_b. À de hauts degrés de saturation (dans une condition non agrégée) $M_a = M_b = M_s$ (le taux de contrainte d'état critique saturé. À des degrés moindres de saturation, la valeur de M_b baisse considérablement et atteint des valeurs proches de zéro avec des degrés de saturation en dessous de 60%. De même, la valeur de M_a semble augmenter á mesure que le degré de saturation baisse. Un comportement similaire est observé pour λ_a et λ_b. Les fonctions mettant en rapport paramètres d'état critique et degré de saturation (ou teneur en eau volumétrique) peuvent être exprimées dans une forme normalisée en les référençant á l'état saturé. Les mêmes fonctions normalisées pour M_a/M_s, M_b/M_s, λ_a/λ_s et λ_b/λ_s correspondent aux données expérimentales pour l'argile sableuse résiduelle de Singapour et pour un gravier latéritique du Kenya testé par Toll (1990). Ceci suggère que la forme de ces fonctions peut être commune á toute une gamme de types de sols.

INTRODUCTION

The critical-state concept has been well established as a useful framework within which saturated soil behaviour can be interpreted (Schofield & Wroth, 1968). The *critical state* is the state achieved by a soil when it exhibits no changes in stress or volume when it is sheared; this is typically achieved at large strains. A soil that is looser (sometimes referred to as *wetter*) than the critical state will contract in volume under shear to achieve the critical state, or if volume change is prevented (an *undrained* condition) then increases in pore water pressure will be generated so that the effective stress state moves towards the critical state. A soil that is denser (or *drier*) than the critical state will dilate, or if volume change is prevented then a decrease in pore water pressure will be generated.

The behaviour of saturated soils is controlled by effective stresses, and for the saturated case water content and volume are interrelated. Therefore the saturated critical state can be expressed through the deviator stress, q, the mean effective stress, p', and the specific volume, v. At the critical state these variables are related through three critical-state parameters, M, Γ and λ:

$$q = Mp' \tag{1}$$

$$v = \Gamma - \lambda \ln p' \tag{2}$$

where M is the slope of the projection of the critical-state line in q–p' space, Γ is the intercept (at $p' = 1$ kPa), and λ is the slope of the projection of the critical-state line in $v - \ln p'$ space.

However, unsaturated soils have an additional phase (the air phase), and it is therefore no longer possible to interpret their behaviour through effective stresses, nor to assume that water content and volume are linked. For unsaturated soils, the stress state can be represented by two stress state variables, the net stress $(\sigma - u_a)$ and the matric suction $(u_a - u_w)$ (Fredlund & Morgenstern, 1977), where u_a is the pore air pressure and u_w is the pore water pressure. In addition to specific volume (or void ratio), the phase state of the soil has to be represented by an additional variable: this can be either gravimetric water content (w), volumetric water content (θ) or degree of saturation (S_r).

Toll (1990) proposed that the critical state for unsaturated soils could be expressed in terms of q, $p - u_a$, $u_a - u_w$, v and S_r. The unsaturated critical state requires five parameters, M_a, M_b, Γ_{ab}, λ_a and λ_w:

$$q = M_a(p - u_a) + M_b(u_a - u_w) \tag{3}$$

$$v = \Gamma_{ab} - \lambda_a \ln(p - u_a) - \lambda_b \ln(u_a - u_w) \tag{4}$$

Note that the contributions due to suction have been labelled M_b and λ_b (rather than the terminology M_w and λ_w originally used by Toll, 1990). This is for consistency with the use of ϕ^b by Fredlund *et al.* (1978) to represent the friction angle for changes in matric suction. The terminology for the

Manuscript received 5 December 2001; revised manuscript accepted 2 October 2002
Discussion on this paper closes 1 August 2003, for further details see p. ii.
* School of Engineering, University of Durham, UK.
† Formerly School of Civil and Structural Engineering, Nanyang Technological University, Singapore.

contributions due to net stress (M_a and λ_a) are already consistent with the use of ϕ^a by Fredlund *et al.* (1978).

Toll (1990) showed that, for a compacted lateritic gravel, M_a, M_b, λ_a and λ_b did not have unique values for unsaturated conditions. It was shown that the variation in the parameters could be expressed as functions of the degree of saturation, S_r. It was argued that it was not degree of saturation *per se* that affected these parameters, but rather the fabric of the soil. Clayey materials compacted dry of optimum moisture content develop an aggregated or 'packet' fabric, and these effects can be observed even in a predominantly granular material that has less than 10% clay. Toll (2000) showed that, for compacted soils, the degree of saturation could give an indication of the amount of aggregation present.

This paper presents test data from triaxial tests on a residual soil from Singapore, tested under unsaturated conditions with measurements of matric suction. The data for critical-state conditions from these tests are presented within the framework proposed by Toll (1990). The critical-state parameters for the Singapore residual soil are established and are compared with the pattern of behaviour for Kiunyu gravel reported by Toll (1990). Their variation is considered with respect to degree of saturation and also volumetric water content.

CRITICAL-STATE STRESS RATIOS FOR UNSATURATED SOILS

Toll (1990) showed that, for a lateritic gravel (Kiunyu gravel), the values of the critical-state stress ratios M_a and M_b varied in a manner that could be expressed as functions of the degree of saturation, S_r. Subsequent research has also identified variations in the critical-state parameters due to changes in suction. The results of tests on compacted kaolin by Zakaria *et al.* (1995) and Wheeler & Sivakumar (1995) showed that the slope of the critical-state line in q, $p - u_a$ space (that is, M_a) increased as suction increased. This would be consistent with an increase in M_a with decreasing degree of saturation (as degree of saturation will reduce as suction increases). It is also consistent with other observations that the friction angle for changes in net stress (that is, ϕ^a) increased with increasing suction (Escario & Saez, 1986), although these latter observations were not made for critical-state conditions. However, Delage *et al.* (1987) and Maâtouk *et al.* (1995) found that, for silts, ϕ^a decreased with increased suction. Ng *et al.* (2000) found that M_a seemed to be constant and independent of the value of suction for two loosely compacted volcanic fills. Nevertheless, their values of M_b did show a clear variation with degree of saturation, similar to that shown by Toll (1990).

Figure 1 shows the functions for M_a and M_b as they relate to degree of saturation for Kiunyu gravel (Toll, 1990). Toll (2000) also expressed the critical-state parameters for Kiunyu gravel in terms of the friction angles ϕ^a and ϕ^b, and a scale for friction angles is shown in Fig. 1. These represent friction angles at the critical state.

At lower degrees of saturation (dry of optimum water content), M_a has greater values than M_s (the stress ratio in saturated conditions). This was explained by Toll (1990, 2000) as being due to the presence of aggregations at lower degrees of saturation, causing the soil to behave in a coarser fashion than would be justified by the grading. In unsaturated conditions the aggregated fabric can be maintained during shear because the suction gives strength to the aggregations. In a saturated soil, any aggregations that did exist would be broken down during shear and would not be expected to affect the critical-state parameters. In any case, samples compacted at high degrees of saturation (above optimum water content) would not be expected to have an aggregated fabric.

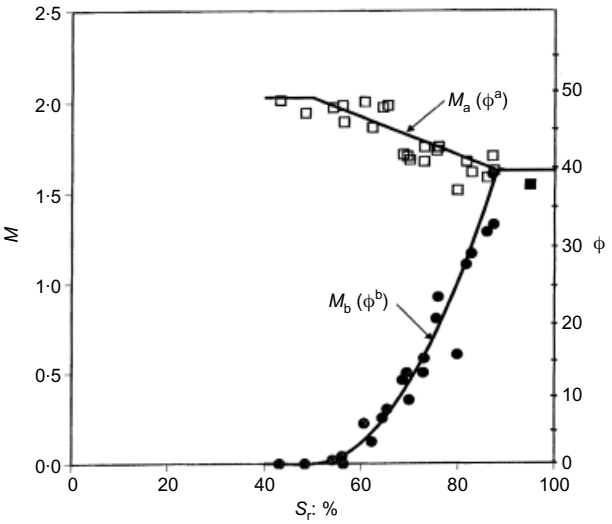

Fig. 1. Variation of critical-state stress ratios with degree of saturation for Kiunyu gravel ($q = M_a(p - u_a) + M_b(u_a - u_w)$)

The same mechanism could explain the drop in ϕ^a for silts observed by Delage *et al.* (1987) and Maâtouk *et al.* (1995). Silty materials would tend to desaturate at much lower suctions. At intermediate values of suction the aggregated fabric would be held together by the suction and could give high angles of friction. However, as the suction increases, the aggregations can progressively desaturate. The desaturated parts would no longer be held together by suction, and would break down. In this case the value of ϕ^a would drop as the aggregated fabric broke down. This same mechanism is likely to affect clayey soils, but at much higher values of suction.

It can be seen from Fig. 1 that, at low degrees of saturation, M_b becomes significantly lower than M_s and eventually drops to zero. It could be that the packet fabric also affects M_b as the water phase withdraws into the packets and suction makes no contribution to the overall strength of the soil. It is also possible that this represents a similar effect to the reduction in the friction angle for suction (ϕ^b) as suction increases, as observed by Escario & Saez (1986) and Fredlund *et al.* (1987). This effect can be explained by a reduction in the area of water over which the suction acts (very like the χ factor used by Bishop, 1959). It has been shown by Fredlund *et al.* (1995) and Vanapalli *et al.* (1996) that the reduction of ϕ^b can be related to normalised volumetric water content or degree of saturation.

The variation in the M_b parameter with degree of saturation has been modelled using a function similar to those used by Vanapalli *et al.* (1996). The function used is

$$\frac{M_b}{M_s} = \left(\frac{S_r - S_{r2}}{S_{r1} - S_{r2}}\right)^k \tag{5}$$

The values for M_b/M_s are numerically very similar to the ratio $\tan\phi^b/\tan\phi'$ (as used by Fredlund *et al.* (1995) and Vanapalli *et al.* (1996)), and can be treated as equivalent, so the same function can be used whether stress ratios or friction angles are being used. The function applies only for $S_{r2} < S_r < S_{r1}$: when $S_r > S_{r1}$ the ratio M_b/M_s is taken as 1·0, and when $S_r < S_{r2}$ it is taken as 0.

Vanapalli *et al.* used full saturation (that is, 100%) as the first reference state, S_{r1}, and the degree of saturation at residual suction as the second reference state, S_{r2}. Here, the two reference states have been chosen to fit the experimental

data. To achieve this, values of $S_{r1} = 88\%$, $S_{r2} = 50\%$ and $k = 2{\cdot}0$ have been used, and the resulting function is shown in Fig. 1. S_{r1} is the point where $M_b = M_s$, and S_{r2} represents the point where $M_b = 0$. The significance of these points will be discussed later. The value of $k = 2{\cdot}0$ provides the required degree of curvature of the function between the two reference states. Fredlund *et al.* (1995) suggested that k should be 1·0 or greater. A value of 2·0 is similar to that used by Vanapalli *et al.* (1996), where typically values of 2·2–2·5 were found to be appropriate for a glacial till.

A similar function has also been used to model the variation in M_a. The function used is

$$\frac{M_a}{M_s} = \left(\frac{M_a}{M_s}\right)_{max} - \left[\left(\frac{M_a}{M_s}\right)_{max} - 1\right]\left(\frac{S_r - S_{r2}}{S_{r1} - S_{r2}}\right)^k \quad (6)$$

This gives a function that varies from $M_a/M_s = 1$ at S_{r1} up to a maximum value of $(M_a/M_s)_{max}$ at S_{r2}. To fit the experimental data, the same values of $S_{r1} = 88\%$ and $S_{r2} = 50\%$ were appropriate (the same values used for fitting M_b) with $(M_a/M_s)_{max} = 1{\cdot}25$. The value of $k = 1{\cdot}0$ was used, since a linear relationship gives a better fit with the experimental data.

CRITICAL-STATE COMPRESSIBILITIES FOR UNSATURATED SOILS

The slopes of the critical-state surface in specific volume space, λ_a and λ_b, like the stress ratios, do not have unique values. Toll (1990) suggested that they can be related to degree of saturation. He also suggested that Γ_{ab} in equation (4) could be related to Γ_s (the intercept for saturated conditions) through the degree of saturation:

$$\Gamma_{ab} = 1 + \frac{\Gamma_s - 1}{S_r} \quad (7)$$

Alonso *et al.* (1990) suggested that the compressibility in v, $p - u_a$ space (in their terminology, $\lambda(s)$) could be related to the value at zero suction ($\lambda(0)$) either through the logarithm of suction or by an exponential function of suction. This would suggest that the compressibility for net stress would reduce as suction increases. Experimental data from Matyas & Radhakrishnan (1968) and Cui & Delage (1996) show this to be the case.

For saturated soils it has been observed that the slope of the critical-state line is parallel to the normal consolidation line. If we assume that this is also true for unsaturated soil, the previous arguments concerning the normal consolidation surface can be applied to the slope of the critical-state line. This would suggest that λ_a would reduce with an increase in suction (that is, it would reduce as the degree of saturation reduces). This is not borne out by the observation of Toll (1990) that λ_a would increase with a reduction in degree of saturation, nor is it supported by other experimental evidence. Wheeler & Sivakumar (1995) found that the slope of the critical-state line in the net stress plane increased as suction increased. Ng *et al.* (2000) showed that λ_a was considerably steeper for a suction of 80 kPa than for the zero suction condition. It is not clear whether this discrepancy means that the slope of the critical-state surface is different from that of the normal consolidation surface, or whether an increase in λ_a with a reduction in degree of saturation (or increase in suction) is due to the fabric of compacted soils.

Figure 2 shows the functions for λ_a and λ_b as they relate to degree of saturation for Kiunyu gravel (Toll, 1990). It was argued that the presence of aggregations (and hence a more open fabric) causes the soil to behave in a more compressible fashion (with respect to net stress) than is justified by the grading. Therefore at lower degrees of saturation (greater aggregation) λ_a had greater values than λ_s (the compressibility in saturated, non-aggregated conditions). At low degrees of saturation λ_b becomes significantly lower than λ_s, and at low water contents drops to zero. This could be due to the packet fabric, reflecting the fact that the water phase withdraws into the packets and suction makes no contribution to the compressibility of the soil. It is also possible that the effect is due to degree of saturation *per se*, reflecting the reduced normalised area of water over which the suction acts, making the suction less effective in causing volume change.

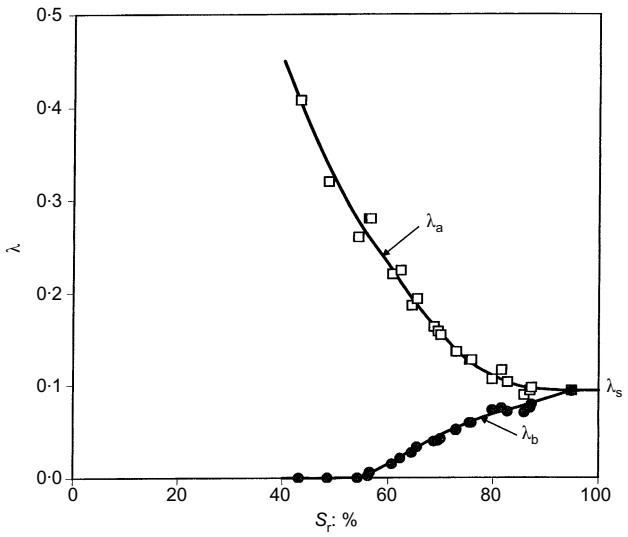

Fig. 2. Variation of critical-state compressibilities with degree of saturation for Kiunyu gravel [$v = \Gamma_{ab} - \lambda_a \ln(p - u_a) - \lambda_b \ln(u_a - u_w)$]

TEST PROGRAMME

Constant water content triaxial tests were carried out on unsaturated samples of the residual soil from Singapore. In addition, consolidated drained tests on saturated samples were performed to define the saturated parameters. The soil tested was obtained from samples taken at a site adjacent to the Nanyang Technological University, School of Civil and Structural Engineering (NTU-CSE), which is located in the Jurong sedimentary deposit of Singapore. Samples were taken from a depth of 4–5 m. Prior to testing, the soil was air-dried for two weeks and passed through a sieve with an aperture size of 2·36 mm. Some classification properties of the soil (after removal of material $< 2{\cdot}36$ mm) are given in Table 1, and the grain size analysis is given in Fig. 3. Comparable information is also given for Kiunyu gravel, tested by Toll (1990).

The Jurong soil was mixed at a water content of 15·6% (1·4% wet of optimum water content) and statically compacted into a mould to obtain specimens of 100 mm height and 50 mm diameter. The intention was to produce specimens with a bulk density of 1·97 Mg/m^3 and a dry density of 1·71 Mg/m^3 (void ratio of 0·6). The compaction was

Table 1. Classification properties

	Jurong residual soil	Kiunyu gravel
Liquid limit: %	36	56–66
Plastic limit: %	22	27–31
Plasticity index: %	15	29–35
Specific gravity of solids	2·72	3·2

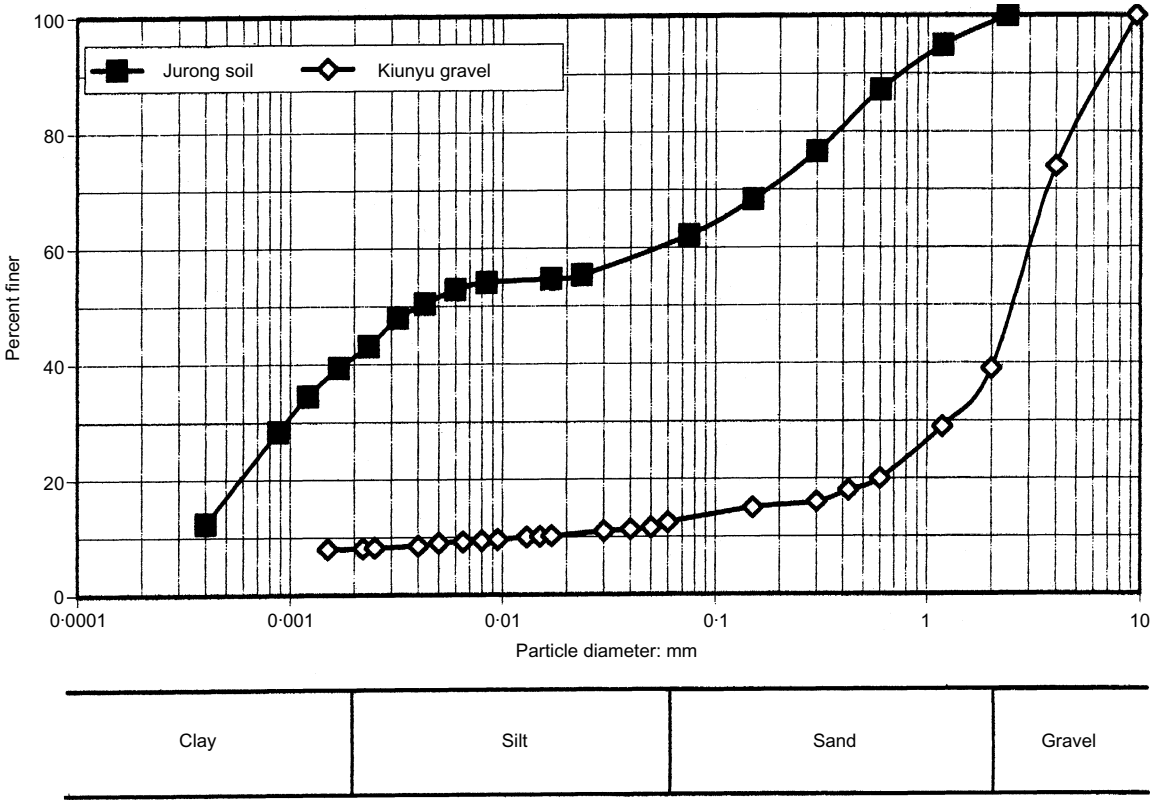

Fig. 3. Particle size distributions for Jurong soil and Kiunyu gravel

carried out in 10 layers, with each layer having an equal thickness of 10 mm. Full details of the specimen preparation are given by Ong (1999).

Three drained triaxial tests were performed on saturated samples of the Jurong soil. The samples were consolidated isotropically to effective confining stresses of 50, 100 and 150 kPa. The shearing rate used was 0·009%/min, the same as that used in the constant water content tests on unsaturated samples. The results are plotted in Fig. 4.

A series of 15 constant water content triaxial tests were carried out on the Jurong soil. The axis-translation technique was used to control and measure the matric suction. In this technique an elevated pore air pressure is used, so that the pore water pressure becomes positive. A high air entry porous disc is used so that the pore water pressure can be measured independently of the pore air pressure. In this test series, a porous ceramic with an air entry value of 500 kPa was used. Pore water pressure was measured at the base of the specimen. A diffused air volume indicator as described by Fredlund & Rahardjo (1993) was used to remove air bubbles from the pore water pressure measuring system before shearing.

After compaction, specimens were initially saturated by applying an elevated back pressure. The specimens were then allowed to equilibrate under appropriate values of isotropic confining pressure, σ_3, pore air pressure, u_a, and pore water pressure, u_w, as shown in Table 2. Net confining stresses $(\sigma_3 - u_a)$ were set at 50, 150 or 250 kPa. Matric suctions $(u_a - u_w)$ varied from 170 to 400 kPa. The specimens were then sheared under constant water content conditions (that is, preventing any flow of water in or out of the specimen). However, the specimens could still change in volume owing to flow of air. The specimen volume was determined by measuring the volume of flow in or out of

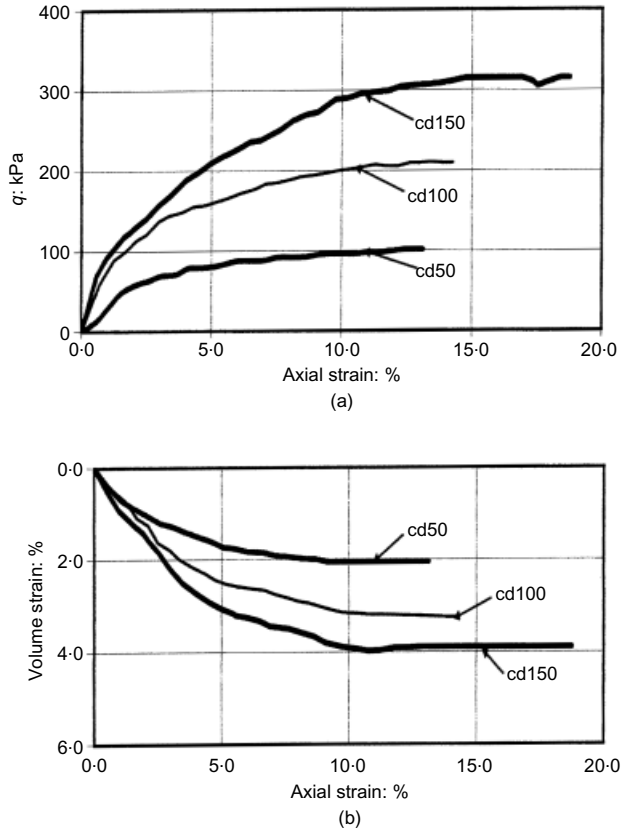

Fig. 4. Results for drained tests carried out on saturated samples, plotted against axial strain: (a) deviator stress, q; (b) volume strain

Table 2. Initial stress values for the constant water content tests

Test	σ_3	u_a	u_w	$\sigma_3 - u_a$	$u_a - u_w$
cw50-170	500	450	280	50	170
cw50-200	500	450	250	50	200
cw50-230 (1)	500	450	220	50	230
cw50-230 (2)	500	450	220	50	230
cw50-250	500	450	200	50	250
cw50-300	500	450	150	50	300
cw50-400	500	450	50	50	400
cw150-220	600	450	230	150	220
cw150-240	600	450	210	150	240
cw150-260	600	450	190	150	260
cw150-300	600	450	150	150	300
cw150-350	600	450	100	150	350
cw150-400	600	450	50	150	400
cw250-280	700	450	170	250	280
cw250-400	700	450	50	250	400

the Perspex triaxial cell surrounding the specimen using a GDS pressure/volume controller. A correction was applied to allow for the downward movement of the loading ram.

A constant strain rate of 0·009%/min was applied to the specimens. This rate was chosen after a pilot study by Ong (1999) showed that this rate (and lower) gave consistent readings of matric suctions in constant water content tests.

The results for tests carried out at a net stress of 50 kPa are plotted in Fig. 5. Similar plots for tests carried out at a net stress of 150 kPa are shown in Fig. 6. The results for tests carried out at a net stress of 250 kPa are shown in Fig. 7.

THE SATURATED CRITICAL STATE FOR JURONG SOIL

The saturated critical state provides a useful reference for the unsaturated critical state. Therefore, initially data from saturated tests and those for constant water content tests that achieved high degrees of saturation (greater than 90% at the end of the tests) will be considered in order to give indications of the saturated critical-state values. At high degrees of saturation the pore air phase exists as occluded air bubbles, and it is acceptable to analyse the soil behaviour from unsaturated tests in terms of effective stresses. This provides additional information to extend the findings obtained from the limited number of tests carried out on saturated samples.

The five constant water content tests that reached high degrees of saturation at the end of the tests were cw50-170, cw50-200, cw150-220, cw150-240 and cw250-280. These tests achieved degrees of saturation between 91% and 93%. Therefore the results of these five tests can be analysed in terms of effective stresses. The results for cw50-170 and cw50-200 (with net stress of 50 kPa and suctions of 170 and 200 kPa respectively) are shown in Fig. 5. Results for cw150-220 and cw150-240 (with net stress of 150 kPa and suctions of 220 and 240 kPa respectively) are shown in Fig. 6, and the result for cw250-280 (with net stress of 250 kPa and suction of 280 kPa) is shown in Fig. 7.

The saturated drained tests (cd50, cd100 and cd150) (Fig. 4) show that both the deviator stress and the volume strain levelled off at axial strains of 12–15%, meaning that a true critical state is achieved. It can be seen that for the constant water content tests, cw50-170 and cw50-200 (Fig. 5), the volume strain shows a tendency to level off at an axial strain above 10%, suggesting that the critical state is being approached. However, the deviator stress and the pore water pressure are still changing towards the end of the tests. A similar picture is seen for cw150-220 (Fig. 6) and cw250-280 (Fig. 7).

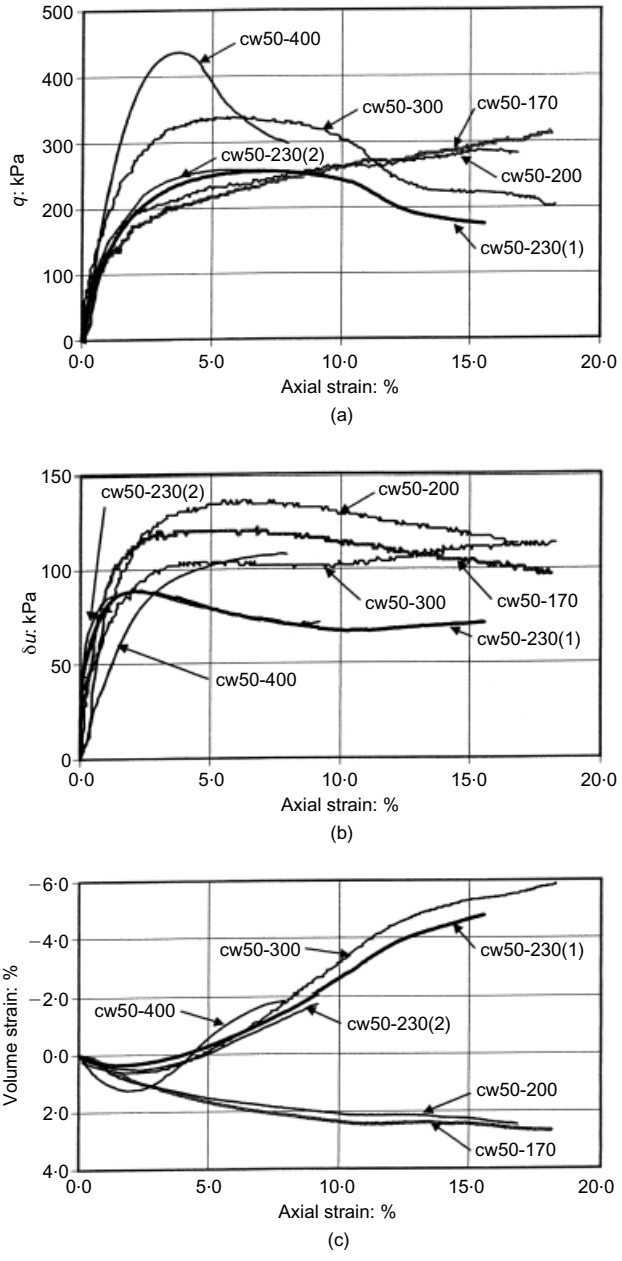

Fig. 5. Results for constant water content tests at net confining stress of 50 kPa and various matric suctions, plotted against axial strain: (a) deviator stress, q; (b) change in pore water pressure, δu; (c) volume strain

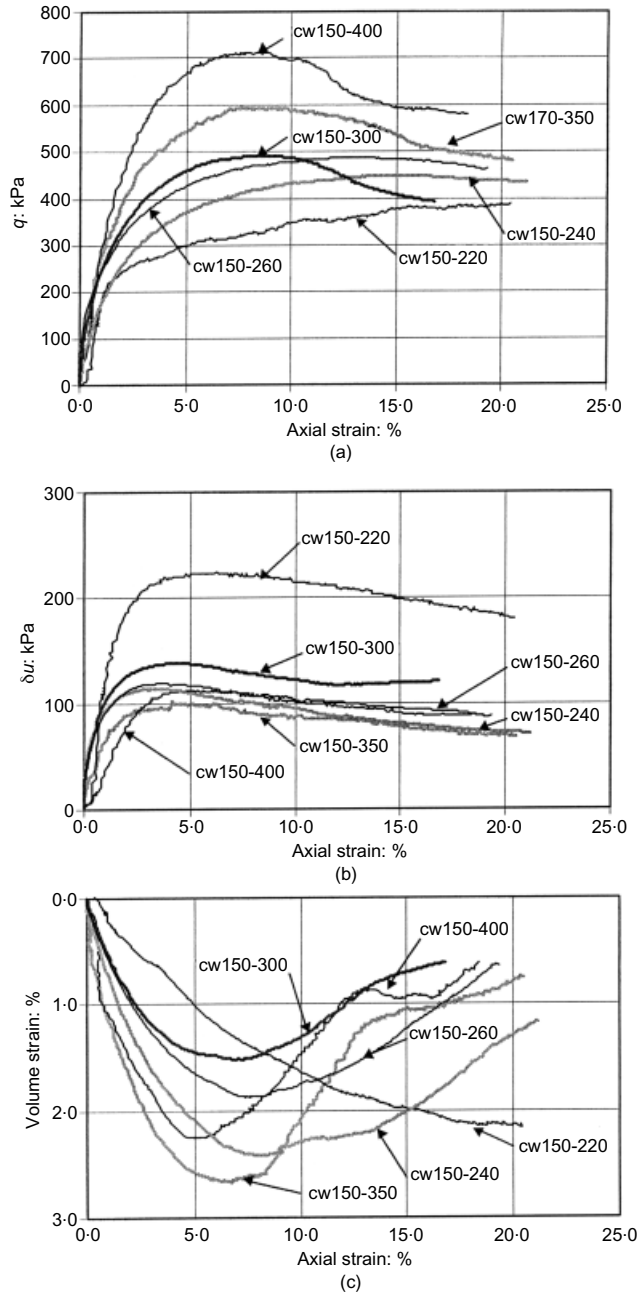

Fig. 6. Results for constant water content tests at net confining stress of 150 kPa and various matric suctions, plotted against axial strain: (a) deviator stress, q; (b) change in pore water pressure, δu; (c) volume strain

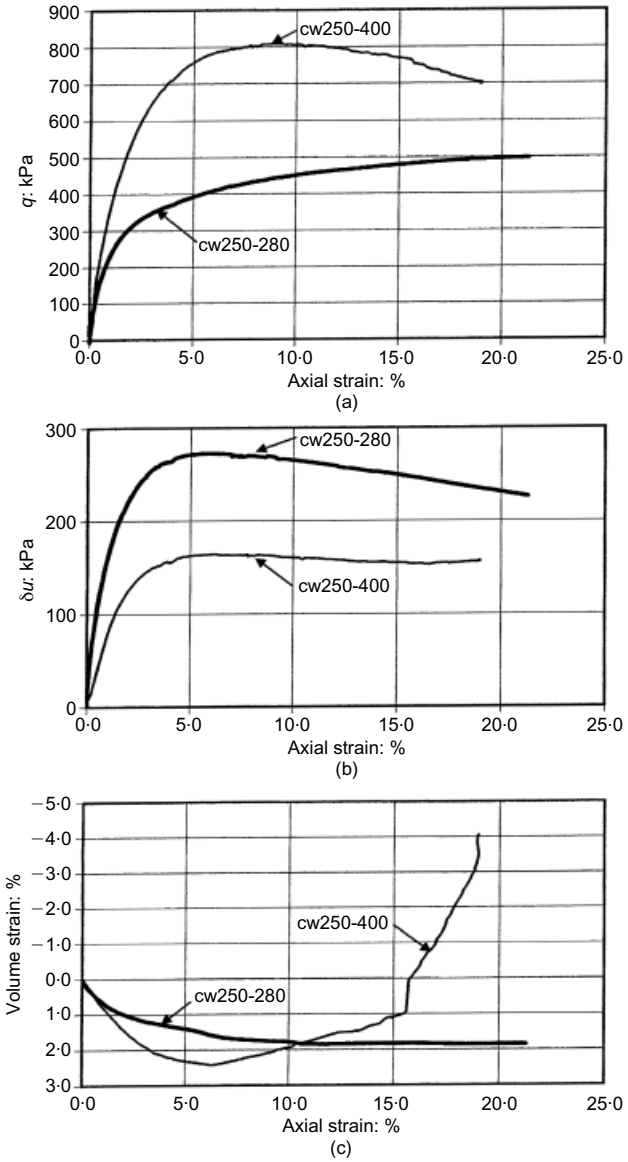

Fig. 7. Results for constant water content tests at net confining stress of 250 kPa and various matric suctions, plotted against axial strain: (a) deviator stress, q; (b) change in pore water pressure, δu; (c) volume strain

A true critical state (that is, no change in deviator stress, pore pressure or volume) was rarely achieved by the end of the constant water content tests. However, the rate of change of these parameters did generally reduce considerably towards the end of the test. In some cases the deviator stress continued to increase (and the pore water pressure to decrease), but by the end of the test the stress path followed a constant stress ratio (q/p'). This can be seen in the stress paths shown in Fig. 8. It is always difficult to define a true critical-state condition for bonded or dense materials as they often fail through the development of distinct shear surfaces, where non-homogeneous deformations (and the possibility for clay particle alignment) will affect the results. Nevertheless, for the purpose of this discussion it will be assumed that the ultimate stress ratio (q/p') defines the critical-state

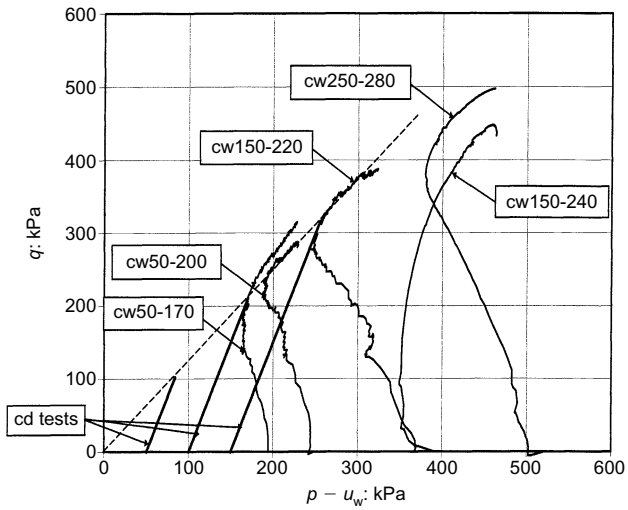

Fig. 8. Stress paths in $q - p'$ space for saturated drained tests and constant water content tests at high degrees of saturation

stress ratio, M. The saturated tests (cd50, cd100, cd150) clearly define M, as they failed in a ductile fashion.

The q/p' ratios for the three saturated drained tests and five constant water content tests at high degrees of saturation are shown in Fig. 9. The saturated drained tests show a consistent ultimate q/p' ratio with a value of 1·23. There is considerable variation in the ultimate stress ratios for the five constant water content tests, as can be seen in Fig. 8. The values range from 0·94 in test cw150-240 to 1·37 in test cw50-170. There does seem to be a trend of reducing q/p' ratio with increasing suction, but with these limited data it is difficult to be sure. It is likely that higher suctions produce more brittle behaviour (and hence the formation of distinct failure surfaces), and this is reflected in the lower q/p' values. However, the ultimate value of q/p' for the saturated drained tests of 1·23 will be taken as the saturated value of M.

The volumetric behaviour of the three saturated drained tests and the five constant water content tests at high degrees of saturation is shown in Fig. 10. The end point of each test is shown by a □ symbol. A line is drawn on the figure representing the projection of the critical-state line (CSL) in e–$\log p'$ space. The line drawn represents values of Γ of 2·0 and λ of 0·08.

The three saturated drained tests (cd50, cd100 and cd150) show contractive behaviour throughout. Similarly, the four constant water content tests that start above the CSL (cw50-170, cw50-200, cw150-220 and cw250-280) show contractive behaviour. Test cw150-240, which starts with a void ratio denser than the critical state, shows strong dilative behaviour in the latter stages of the test. This difference in state for test cw150-240 (that is, starting below the CSL) explains why this test shows such a different stress path in Fig. 8.

In conclusion, the test results for saturated tests and those at high degrees of saturation provide values for the saturated critical-state parameters of $M = 1{\cdot}23$, $\Gamma = 2{\cdot}0$ and $\lambda = 0{\cdot}08$.

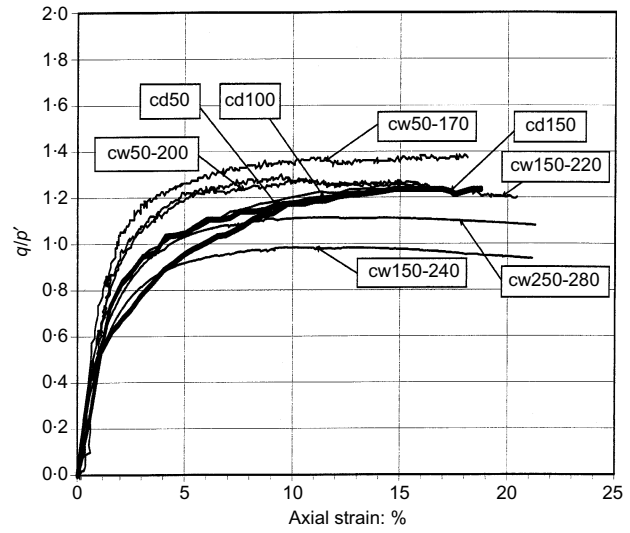

Fig. 9. Stress ratio, q/p', plotted against axial strain for saturated drained tests and constant water content tests at high degrees of saturation

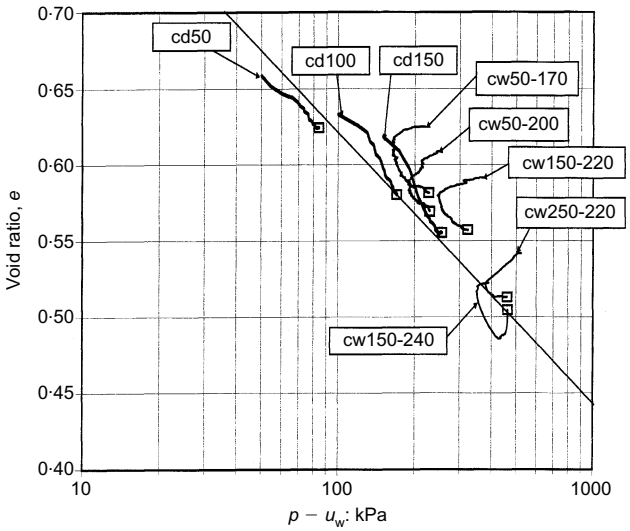

Fig. 10. Void ratio, e, plotted against p' for saturated drained tests and constant water content tests at high degrees of saturation

THE UNSATURATED CRITICAL STATE FOR JURONG SOIL

Table 3 shows the values of the stress state variables (q, $p - u_a$ and $u_a - u_w$) and the phase state variables (w, e and S_r) at the end of each test. It can be seen that the degree of saturation at the end of the tests varies from 93% down to 61%.

By examining the values of q, $p - u_a$ and $u_a - u_w$ it is possible to assess values of M_a and M_b from equation (3). It was assumed that these values would relate to the degree of saturation, as suggested by Toll (1990). An initial assumption was made that M_a was constant and equal to M_s, independent of S_r. Values of M_b were then determined so that the predicted value of deviator stress, q, calculated from equation (3) (based on the observed values of $p - u_a$ and $u_a - u_w$) was equal to the observed value of q. This initial assessment gave a distribution of values of M_b that did not show a consistent function with degree of saturation. The values of M_a were then adjusted by trial and error and new values of M_b calculated so that reasonably consistent functions of both M_a and M_b were achieved. The results of this assessment are shown in Fig. 11.

Although there is some scatter in Fig. 11, the predominant trends are reasonably clear. The values of M_a and M_b for the tests at high degrees of saturation are seen to be equal to each other, and range from 0·94 to 1·37, scattering around the value for M_s of 1·23 as discussed in the previous section. As the degree of saturation reduces, the values of M_b drop considerably, and reach values less than 0·1 at a degree of saturation near 60%. Conversely, the values of M_a appear to increase with reducing degree of saturation. This is consistent with the pattern observed by Toll (1990).

The functions shown by lines in Fig. 11 are given by equation (5) using the same values of $S_{r1} = 88\%$, $S_{r2} = 50\%$ and $k = 2{\cdot}0$ as used for Kiunyu gravel, but are now based on an M_s value of 1·23 appropriate for the Jurong soil. It can be seen that the functions give a very reasonable fit to the data obtained for the Jurong sedimentary soil. This suggests that the form of the function may be common to a range of soil types, as the same form fits both a lateritic gravel and a residual sandy clay. These functions, expressed as the normalised variables M_a/M_s and M_b/M_s, are plotted in Fig. 12.

By examining the values of e, $p - u_a$ and $u_a - u_w$ it is possible to assess values of λ_a and λ_b from equation (4). Values of Γ_{ab} were calculated from the value of Γ_s and S_r using equation (7). As before, it was assumed that the values of λ_a and λ_b would relate to the degree of saturation. The same process used to determine M_a and M_b was used to

Table 3. End of test values for the stress and phase variables.

Test	q	$p - u_a$	$u_a - u_w$	w	e	S_r
cw50-170	311	154	73	19·4	0·581	90·5
cw50-200	283	144	85	19·2	0·569	91·7
cw50-230(1)	175	108	158	16·7	0·686	66·3
cw50-230(2)	247	132	158	16·7	0·637	71·3
cw50-250	332	161	182	16·2	0·692	63·8
cw50-300	204	118	186	14·6	0·628	63·1
cw50-400	298	150	292	14·1	0·528	72·3
cw150-220	385	278	44	18·7	0·557	91·0
cw150-240	433	294	168	17·0	0·505	91·6
cw150-260	463	304	171	16·5	0·607	74·0
cw150-300	391	280	178	15·9	0·583	74·3
cw150-350	480	310	282	14·5	0·481	82·1
cw150-400	579	343	311	13·3	0·583	61·9
cw250-280	497	416	45	17·6	0·513	93·0
cw250-400	699	483	241	14·5	0·649	60·9

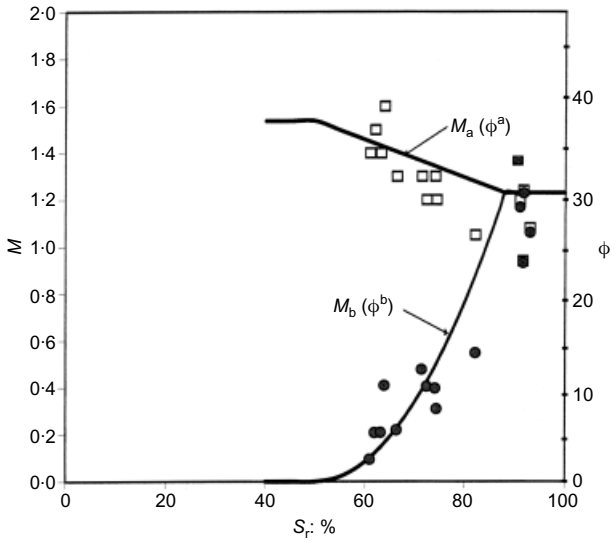

Fig. 11. Variation of critical-state stress ratios with degree of saturation for Jurong soil [$q = M_a(p - u_a) + M_b(u_a - u_w)$]

determine the functions for λ_a and λ_b. The results of the assessment are given in Fig. 13.

The functions shown by lines in Fig. 13 are the same functions as observed for Kiunyu gravel (Fig. 2) but re-plotted for a λ_s value of 0·08. It can be seen that the functions correspond very closely to the data obtained for the Jurong sedimentary soil. Like the functions for M_a/M_s and M_b/M_s, this suggests that the form of the functions for λ_a/λ_s and λ_b/λ_s may be common to a range of soil types. These functions, expressed as the normalised variables λ_a/λ_s and λ_w/λ_s, are plotted in Fig. 14.

FUNCTIONS USING VOLUMETRIC WATER CONTENT

The functions for the critical-state stress ratios, expressed as the normalised variables M_a/M_s and M_b/M_s (Fig. 12), have so far been expressed in terms of degree of saturation using equations (5) and (6). The form of these functions has also been investigated in terms of volumetric water content. This has the advantage that it can be related to the soil–water characteristic curve when expressed in terms of volumetric water content, an approach that has been favoured by

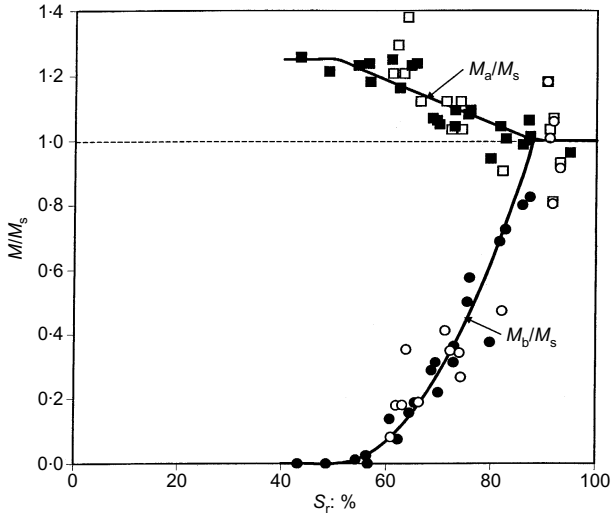

Fig. 12. Normalised functions for critical-state stress ratios (solid symbols, Kiunyu gravel; open symbols, Jurong soil)

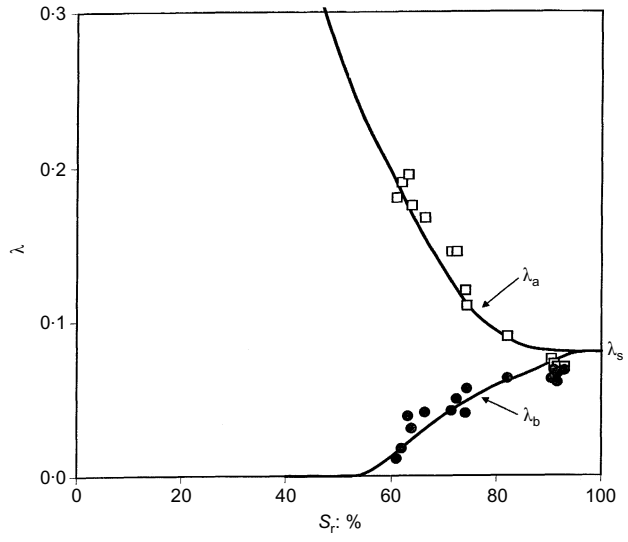

Fig. 13. Variation of critical-state compressibilities with degree of saturation for Jurong soil [$v = \Gamma_{ab} - \lambda_a \ln(p - u_a) - \lambda_b \ln(u_a - u_w)$]

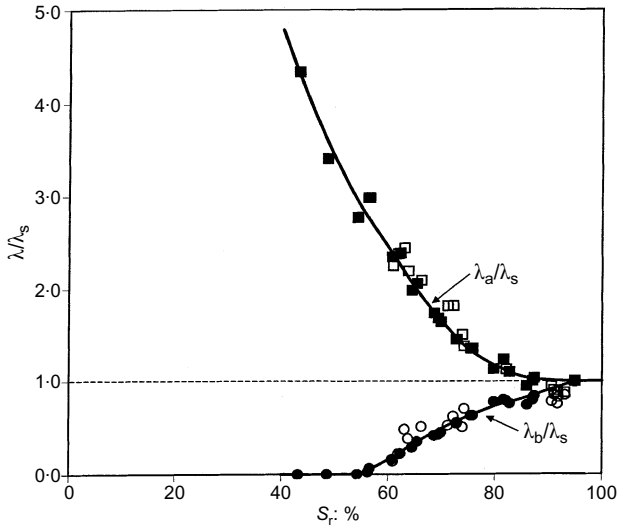

Fig. 14. Normalised functions for critical-state compressibilities (solid symbols, Kiunyu gravel; open symbols, Jurong soil)

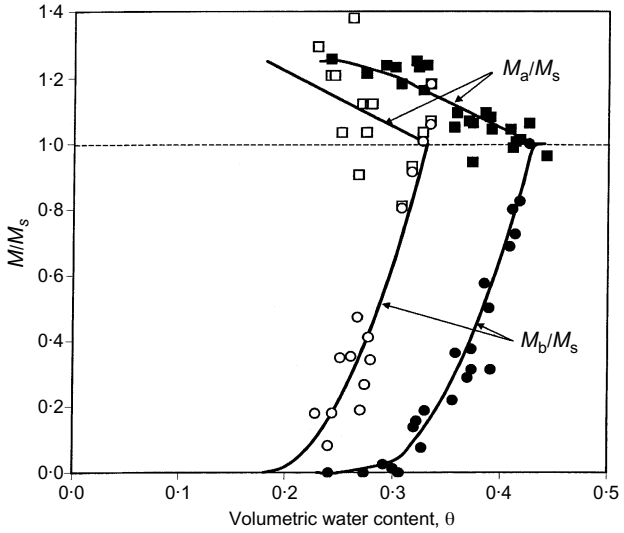

Fig. 15. Variation of critical-state stress ratios with volumetric water content (solid symbols, Kiunyu gravel; open symbols, Jurong soil)

Fredlund *et al.* (1995) and Vanapalli *et al.* (1996). They suggested that

$$\frac{\tan\phi^{b}}{\tan\phi'} = \Theta^{k} = \left(\frac{\theta - \theta_{r}}{\theta_{s} - \theta_{r}}\right)^{k} \tag{8}$$

A similar approach will be used here, represented by the function:

$$\frac{M_{b}}{M_{s}} = \Theta^{k} = \left(\frac{\theta - \theta_{p2}}{\theta_{p1} - \theta_{p2}}\right)^{k} \tag{9}$$

The values of θ_{p1} and θ_{p2} are chosen as the best fit for the experimental data. Their significance will be discussed in the following.

The M_a values were modelled using the following function (similar to equation (6)):

$$\frac{M_{a}}{M_{s}} = \left(\frac{M_{a}}{M_{s}}\right)_{max} - \left[\left(\frac{M_{a}}{M_{s}}\right)_{max} - 1\right]\Theta^{k} \tag{9}$$

The values of θ_{p1} and θ_{p2} that best fitted the Kiunyu gravel data (for both M_b and M_a) were $\theta_{p1} = 0{\cdot}27$ and $\theta_{p2} = 0{\cdot}43$. For the Jurong soil, $\theta_{p1} = 0{\cdot}18$ and $\theta_{p2} = 0{\cdot}33$. In both cases a value of $k = 2{\cdot}0$ was used for M_b and $k = 1{\cdot}0$ for M_a (the same values as used for fitting degree of saturation data). The results are plotted in terms of volumetric water content in Fig. 15, and can be seen to give a realistic fit to the data. The data for both materials are also plotted in terms of normalised water content, Θ, in Fig. 16. The curvature of the M_b function can be clearly seen (modelled with $k = 2{\cdot}0$) compared with the linear function for M_a (using $k = 1{\cdot}0$). It can be seen that both sets of data fit the same functions in terms of normalised volumetric water content, as did the degree of saturation functions (Fig. 12).

Soil–water characteristic curves determined from pressure plate tests are shown for both Kiunyu gravel and Jurong soil in Fig. 17. The test equipment in both cases was limited to a maximum matric suction of 500 kPa. This means that the residual suction cannot be defined as it is clear that both soil–water characteristic curves continue to show significant changes in volumetric water content up to the limit of the test data. However, the curve for the Jurong soil does show the slope of the curve decreasing at suctions above 200 kPa.

The values of θ_{p1} and θ_{p2} for the Jurong soil have been indicated in Fig. 17. It can be seen that θ_{p1} is close to the

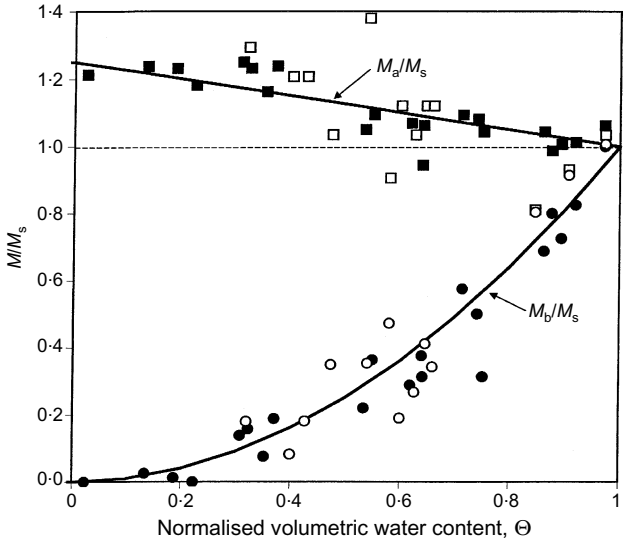

Fig. 16. Variation of critical-state stress ratios with normalised volumetric water content (solid symbols, Kiunyu gravel; open symbols, Jurong soil)

air entry value for the soil, possibly representing the end of the *boundary effect zone* and the start of the *primary transition zone* as defined by Vanapalli *et al.* (1996). θ_{p2} coincides with the break in slope of the curve at 200 kPa, possibly representing the end of the primary transition zone.

Unfortunately, the limit on suction for the test on Kiunyu gravel means that only the initial part of the curve is identified. The value of θ_{p1} is shown and falls on the initial part of the soil–water characteristic, again possibly representing the start of the primary transition zone. The value of θ_{p2} falls outside the experimental results, so no conclusions can be drawn for the Kiunyu gravel.

It is clear that the two reference states (θ_{p1} and θ_{p2}) needed to define the function for variations in the stress ratios do not coincide with saturation (θ_s) and residual conditions (θ_r), as suggested by Fredlund *et al.* (1995) and Vanapalli *et al.* (1996). From the limited information on soil–water characteristic curves it would seem that the limits

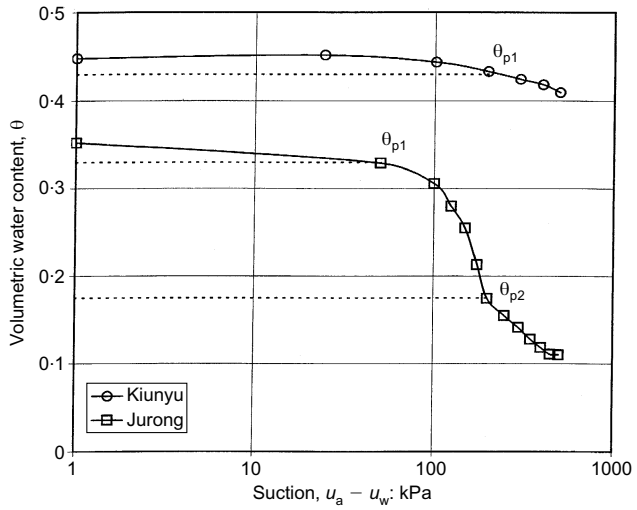

Fig. 17. Soil–water characteristic curves for Kiunyu gravel and Jurong soil

of volumetric water content appropriate for normalisation could be defined by the start and end of the primary transition zone.

CONCLUSIONS

The critical state for unsaturated soils can be expressed in terms of the following variables: deviator stress, q; net mean stress, $p - u_a$; matric suction, $u_a - u_w$; specific volume, v; and degree of saturation, S_r. The unsaturated critical state requires five parameters: M_a, M_b, Γ_{ab}, λ_a and λ_b. These can be referenced to the saturated critical-state parameters M_s, Γ_s and λ_s. The variation in critical-state stress ratios (M_a and M_b) and the critical-state compressibilities (λ_a and λ_b) can be expressed as functions of the degree of saturation of the soil.

Results from constant water content tests on unsaturated samples of soils from the Jurong residual soil in Singapore have been used to determine the critical-state parameters for the soil in an unsaturated state. Tests on saturated specimens indicate saturated critical-state parameters of $M_s = 1{\cdot}23$, $\Gamma_s = 2{\cdot}0$ and $\lambda_s = 0{\cdot}08$. At high degrees of saturation $M_a = M_b = M_s$. At lower degrees of saturation the value of M_b drops considerably, and reaches a value near to zero at degrees of saturation below 60%. Conversely, the value of M_a appears to increase with reducing degree of saturation. This is consistent with the pattern observed by Toll (1990).

A similar pattern is observed for λ_a and λ_b. At high degrees of saturation $\lambda_a = \lambda_b = \lambda_s$. As the degree of saturation reduces the value of λ_b drops, and reaches a value near to zero at degrees of saturation below 60%. Conversely, the value of λ_a clearly increases significantly with reducing degree of saturation, as observed by Toll (1990).

The functions relating the critical-state parameters to degree of saturation can be expressed in normalised form by referencing them to the saturated state. The same normalised functions for M_a/M_s, M_b/M_s, λ_a/λ_s and λ_b/λ_s fit the experimental data for the Jurong residual soil from Singapore and also the data for a lateritic gravel from Kenya reported by Toll (1990). This suggests that the form of these functions may be common to a range of different soil types.

The functions can also be expressed in terms of normalised volumetric water content. It seems from limited data that the two reference states needed for normalisation may be defined by the start and end of the primary transition zone identified from the soil–water characteristic curve.

ACKNOWLEDGEMENTS

Both authors would like to acknowledge the role of Associate Professor H. Rahardjo of Nanyang Technological University (NTU), Singapore, in facilitating this research. Associate Professor Rahardjo was instrumental in arranging for Dr Toll to spend two years at NTU as a research fellow, and he was the supervisor for Mr Ong's MEng studies.

NOTATION

e	void ratio
k	fitting parameter used for relating shear strength to Θ (Fredlund *et al.*, 1995)
M, M_s	critical-state stress ratio for saturated conditions ($= q/p'$)
M_a	critical-state stress ratio for changes in net mean stress ($p - u_a$)
M_b	critical-state stress ratio for changes in matric suction ($u_a - u_w$)
p	mean stress ($= (\sigma_1 + \sigma_2 + \sigma_3)/3$)
q	deviator stress ($= \sigma_1 - \sigma_3$)
S_r	degree of saturation
u_a	pore air pressure
u_w	pore water pressure
δu	change in pore water pressure
v	specific volume ($= 1 + e$)
w	gravimetric water content
Γ, Γ_s	critical-state intercept for volumetric plane at $p' = 1$ kPa for saturated conditions
Γ_{ab}	critical-state intercept for volumetric planes at $p - u_a = 1$ kPa and $u_a - u_w = 1$ kPa
θ	volumetric water content
θ_s	volumetric water content at saturation
θ_r	volumetric water content at residual suction
θ_{p1}	volumetric water content at start of primary transition zone
θ_{p2}	volumetric water content at end of primary transition zone
Θ	normalised volumetric water content
λ, λ_s	slope of critical-state line in v–$\ln p'$ plane for saturated conditions
λ_a	slope of critical-state line in v–$\ln(p - u_a)$ plane
λ_b	slope of critical-state line in v–$\ln(u_a - u_w)$ plane
σ	total stress
ϕ^a	angle of friction for changes in net stress ($\sigma - u_a$)
ϕ^b	angle of friction for changes in matric suction ($u_a - u_w$)

REFERENCES

Alonso, E. E., Gens, A. & Josa, A. (1990). A constitutive model for partially saturated soils. *Géotechnique* **40**, No. 3, 405–430.

Bishop, A. W. (1959). The principle of effective stress. *Teknisk Ukeblad* **106**, No. 39, 859–863.

Cui, Y. J. & Delage, P. (1996). Yielding and plastic behaviour of an unsaturated compacted silt. *Géotechnique* **46**, No. 2, 291–311.

Delage, P., Suraj de Silva, G. P. R. & de Laure, E. (1987). Un nouvel appareil triaxial pour les sols non saturés. *Proc. 9th Eur. Conf. Soil Mech. Found. Engng, Dublin* **1**, 25–28.

Escario, V. & Saez, J. (1986). The shear strength of partly saturated soils. *Géotechnique* **36**, No. 3, 453–456.

Fredlund, D. G. & Morgenstern, N. R. (1977). Stress state variables for unsaturated soils. *Can. Geotech. J.* **16**, 121–139.

Fredlund, D. G. & Rahardjo, H. (1993). *Soil mechanics for unsaturated soils.* New York: Wiley.

Fredlund, D.G., Morgenstern, N. R. & Widger, R. A. (1978). The shear strength of unsaturated soils. *Can. Geotech. J.* **31**, 533–546.

Fredlund, D. G., Rahardjo, H. & Gan, J. K.-M. (1987). Nonlinearity of strength envelope for unsaturated soils. *Proc. 6th Int. Conf. Expansive Soils, New Delhi*, 49–54.

Fredlund, D. G., Xing, A., Fredlund, M. D. & Barbour, S. L. (1995). The relationship of the unsaturated soil shear strength to the soil-water characteristic curve. *Can. Geotech. J.* **32**, 440–448.

Maâtouk, A., Leroueil, S. & La Rochelle, P. (1995). Yielding and critical state of a collapsible unsaturated silty soil. *Géotechnique* **45**, No. 3, 465–477.

Matyas, E. L. & Radhakrishnan, H. S. (1968). Volume change characteristics of partially saturated soils. *Géotechnique* **18**, No. 4, 432–448.

Ng, C. W. W., Chiu, C. F. & Rahardjo, H. (2000). Laboratory study of loosely compacted unsaturated volcanic fill. In *Unsaturated soils for Asia* (eds H. Rahardjo, D. G. Toll and E. C. Leong), pp. 551–556. Rotterdam: Balkema.

Ong, B. H. (1999). *Shear strength and volume change of unsaturated residual soil*. MEng Thesis, School of Civil and Structural Engineering, Nanyang Technological University, Singapore.

Schofield, A. W. & Wroth, C. P. (1968). *Critical state soil mechanics*. London: McGraw-Hill.

Toll, D. G. (1990). A framework for unsaturated soil behaviour. *Géotechnique* **40**, No. 1, 31–44.

Toll, D. G. (2000). The influence of fabric on the shear behavior of unsaturated compacted soils. In *Advances in unsaturated soils* (eds C. Shackelford, S. L. Houston and N.-Y. Chang), pp. 222–234. Reston: American Society of Civil Engineers, Geotechnical Special Publication No. 99.

Vanapalli, S. K., Fredlund, D. G., Pufahl, D. E. & Clifton, A. W. (1996). Model for the prediction of shear strength with respect to soil suction. *Can. Geotech. J.* **33**, 379–392.

Wheeler, S. J. & Sivakumar, V. (1995). An elasto-plastic critical state model for unsaturated soil. *Géotechnique* **45**, No. 1, 35–53.

Zakaria, I., Wheeler, S. J. & Anderson, W. F. (1995). Yielding of unsaturated compacted kaolin. *Proc. 1st Int. Conf. on Unsaturated Soils,* Paris, Rotterdam: Balkema (eds E. E. Alonso and P. Delage), **1**, 223–228.